Int. J. Nanoelectronics and Materials **9** (2016) 17-36

Structural and optical properties of TiO_2 nanoparticles/PVA for different composites thin films

A.M.Shehap and Dana S.Akil*

Department of Physics, Faculty of Science, Cairo University, Giza , Egypt.

Received 31 March 2015; Revised 28 May 2015; Accepted 3 June 2015

Abstract

Polymeric films based on polyvinyl alcohol (PVA) doped with titanium dioxide nanoparticles at different weight percentage (1.25, 2.5, 5, 7.5, 10 TiO_2/PVA) were prepared using the sonification and casting techniques. The structural properties of those samples were examined by XRD, FTIR, and UV-Visible .The XRD pattern revealed that the amorphous domain in PVA polymer matrix increased with raising the TiO_2 content. The complexation of the dopant with the polymer was examined by FTIR studies .The absorption spectra of UV-Visible light showed irregular changes of the absorption for high doping samples in UV range (7.5, 10 TiO_2 /PVA). Absorbance, transmittance and reflectance spectra were used for the determination of the optical constants. The results indicated that the optical band gap decreases with increasing TiO_2 content, while the refractive index increased to high value for the composites of high dopant. Using the Wemple-DiDomenico model, we calculated the static reflection index, the oscillation energy, and the dispersion energy. The dispersion energy changes slowly as a function of TiO_2 percentage .The dispersion parameters and the high frequency dielectric constant were determined. In addition the average oscillator wavelength λ_0 and oscillator strength S_0 for the investigated samples were found to be strongly affected by the nanopartices dopant.

Keywords : PVA, TiO_2, XRD, FTIR, UV-visible, Wemple-DiDomenico.
PACS: 78.66.-w,78.66.5q

1. Introduction

In recent years, nanocomposite materials have received great interest for both industrial and academic applications [1]. Addition of a small amount of nanomaterial could improve the performance of polymeric materials because of their small size, large specific surface area, quantum confinement effects and strong interfacial interactions [2]. Among these polymers, Poly (vinyl alcohol) (PVA) is a polymer that has been studied intensively because of its good film forming and physical properties, high hydrophilicity, processability, biocompatibility, and good chemical resistance[3]. It is a semi-crystalline polymer, containing crystalline and amorphous phase. When such a polymer is doped with a suitable dopant, it may interact either in the amorphous fraction or in the crystalline fraction of the polymer and in both cases its different physical quantities are changed depending upon the structural change. Hence the complete information about the effect of additives on a specific polymer helps in tailoring those polymer properties for a particular application [4].

Many kinds of nanomaterials have been used to prepare organic/inorganic nanocomposites among these inorganic fillers, TiO_2 nanoparticles have a special place because of its good stability, high refractive index**,** hydrophilicity, UV absorbance, nontoxicity and excellent transparency for the visible light. TiO_2 is well known as a matter with strong redox ability and used for photo electrochemical cell [5], water or air purification [6], to degrade the organic pollutants killing the bacteria due, high photocatalytic activity and low cost [7]. It can be found mainly as a pigment in powder form, providing whiteness to products such as paints, papers, coating plastics, food packaging material, ink, cosmetics and so on [8]. For all these applications, particle size and good dispersion of the TiO_2 nanoparticles in polymer matrix are very important factors. Many preparation methods are used to fabricate the nanocomposite among them the casting method, which is widely used in the preparation processes for inorganic/organic composite**.** The advantage of this method is that the synthesis process is done at room temperature and the organic polymer can be introduce at the initial stage in which the particles of solution kept in the homogenous dispersed state. The addition of the in organic particle in the polymer matrices arise a new composite material which greatly differs from conventional material .TiO_2 nanoparticles can be directly added in organic coating, but due to the high surface area and high polarity, there is a strong tendency for them to aggregate. Therefore, in order to improve the homogeneous dispersion of nanoparticles many researchers have been focused upon using ultrasonic irradiation.

The ultrasonic radiation is more effective than mechanical stirring because it produces strong shock waves at solid liquid interface leading to quick reaction. Also, it produces a transient cavity and asymmetry collapse in very short time which is called ultrasonic cavitations. These collapses set up micro-jet which impact solid surface to accelerate mass transfer and to make the solid surface active. The mass transfer and diffusion are accelerated because of the intensive mass motion caused by ultrasonic, which makes the mass stripped the surface and the surface is uploaded [9]. It is found that the basal spacing(d) of the solid can be expanded in short time as detected from the XRD, so ultrasonic irradiation time can markedly affect the increasing extend of basal spacing [10]. Based on sonochemical theory the ultrasonication of liquid could generate hot spots as high as 5000^{o} K and local pressure as high as 500 atm, also heating and cooling rate greater than 10^{o} K/s. Therefore ultrasonic irradiation can produce a very harsh environment that can induce same chemical reactions that cannot take place under usual condition and could be extensively applied to approach homogeneous dispersion of nanoparticles in organic polymer. It has been reported that high intensity ultrasonic could exceed the attractive force of molecules to produce high concentrations of H and OH radicals in water. Meanwhile, continuing ultrasound leads to degradation of polymer chains, resulting in low molecular weight at the end.

The object of this work is to prepare TiO_2/PVA nanocomposite films with different composition ratios of the two materials (1.25, 2.5, 5, 7.5 and 10 wt%TiO_2). Ultrasonic was used as a major factor for preparation in order to get better dispersion. The obtained films were characterized by different spectroscopic methods such as XRD, FTIR and UV-Vis spectroscopy taking in consideration the application of single oscillator to evaluate the changes in the resulting nanocomposites.

2. Experimental

The polymer nanocomposte films were prepared by casting technique with the aid of ultrasonic irradiation .Casting method based on liquid particle dispersion, where the water was used as PVA polymer solvent, then the polymer solution used as nanoparticles dispersant. Once we get a homogeneous dispersed mixture, the solvent evaporate yields a homogeneous nanocomposite solid film. Since the nanoparticles tends to agglomerate ,the ultrasonic radiation were employed to get a good dispersion of the TiO2 nanoparticles in the PVA solution .Ultrasonic produces a harsh environment for some chemical interaction to take place between the polymer and the nanoparticles which would result in a better dispersion and less agglomeration

2.1 Materials

All chemicals and materials were obtained and used as received without further purification Poly vinyl alcohol with MW= 15000(Sigma Aldrich), TiO_2 nanoparticles with particle size about 25 nm (CMRDI) Helwan, Cairo, Egypt) .The deionized (DI) water was used in the samples preparation

2.2 Preparation of TiO_2/PVA nanocomposite film:

Pure PVA film: The appropriate weight of PVA (1gm) was dissolved in 100 ml of DI water. The mixture was magnetically stirred continuously and heat (80^oC) for 4 hours, until the solution mixture becomes a homogenous viscous appearance at room temperature. The gel is poured into Petri dish and left for 3 days to solidify at room temperature .The thickness of the final film was bout (50μm).

TiO_2/PVA naocomposites: 1g of PVA was dissolved in the same approach above. Different weight percentage of TiO_2 nanoparticles were added to water and magnetically stirred vigorously for 3hours and sonicated using ----- for 1 hour to prevent the nanoparticles agglomeration .The mixture were mixed with the PVA solution and magnetically stirred for 2 hours then sonicated for 1 hour to get good dispersion without agglomeration . The final PVA /TiO_2 mixture were cast in glass Petri dish , air bubbles were removed by shaking and blowing air and were left until dry .This procedure were repeated to make (1.25%,2.5%,5%,7.5%,10%,12.5% TiO_2/PVA composites) .The films were about 50 μm in thickness. The thicknesses of films were controlled by using the same amount of total materials and the same glass Petri dish size.

3. Measuring Techniques

*X-ray spectroscopy:*X-ray diffraction patterns were obtained using advanced refraction system XRD Scintag Ins., USA. The tube used was Copper radiation and the filter was Nickel. The relative intensity was recorded in scattering over an angular angle (2θ) of $4\text{-}50^o$.

*Infrared spectroscopy:*The infrared spectral analysis (IR) of the samples was carried out using PYE Unican spectrophotometer over the range 400-4000 cm-1.

*Ultraviolet/visible spectroscopy:*The ultraviolet/visible absorption spectra of the samples under investigation were recorded on a Perkin Elmer 4B spectrophotometer over the range 190-1100 nm.

4. Results and Discussion

4.1 X ray diffraction (XRD)

The X-ray diffraction measurement has been done to investigate the nanostructure and crystalinity of pure and TiO_2/ PVA polymer nanocomposites. Fig.1 shows XRD of Pure PVA, Pure TiO_2 nanoparticle of anatase type and their composites (1.25, 2.5, 5, 7.5 and 10 wt/wt /PVA) in the angle range of 2θ=5-70 °. The pure PVA the spectrum shows a broad peak between 2θ equates to 15 ° up to 30 °, which contains the crystalline and amorphous regions [11]. While the pure TiO_2 the spectra shows the peaks that characterizes the pattern of the crystalline anatase similar to those found in literature [12]

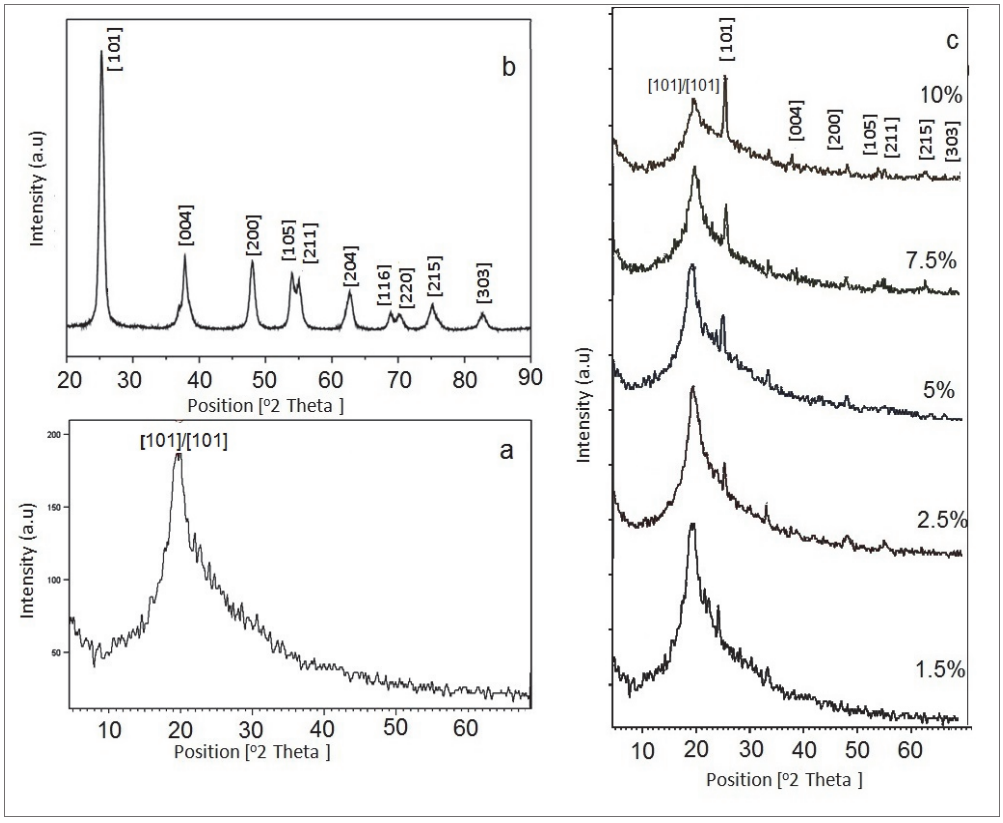

Fig. 1: X-ray diffraction pattern for (a) Pure PVA (b) Pure TiO_2 (c) TiO_2/PVA composites.

However, in the doped films 1.25% and 2.5% TiO_2 /PVA , the peak of PVA (2θ=19.8$^{o)}$ can be observed in the samples along with only one Peak of Tio2 ,the most intense , (2θ=25.3) in addition to another new peak at 2θ=32^o ,which have not been observed in pure PVA or in pure TiO_2. These means the nanoparticles has been dissociated during the stirring by the ultrasonic waves and an interaction occurred between PVA and TiO_2 indicated by the appearance of this new peak at 2θ=32$^{o.}$ The other doped samples (5%, 7.5%, 10% TiO_2 /PVA wt/wt) did not lead to disappearance of the any of the indexed peaks of nanoparticles , but in the same time accompanied with new peak at 2θ=32^o i.e. the doped samples have new modified structure. On the other hand the region of XRD concerning the semi crystalline of PVA, has been changed according to the percentage of loading of TiO_2 .Certainly in the doped films the peak of PVA has been found to be increased in broadness and decreased in intensity, which indicate an increasing in the amorphous region

of PVA in the doped films after doping with TiO_2 .The numbers of hydrogen bonds are formed between the layers of PVA are responsible for the crystallization of the polymer. So the interaction between PVA chains and TiO_2 particles (via hydroxyl bonds) led to the decrease of intermolecular interaction of PVA chains, which would result in decreasing the crystalline degree of PVA depending on the loading of TiO_2 and its homogeneity of dispersion in the composites samples. The possibility of interaction between PVA and TiO_2 is resulted due to that Ti^+ ions interacted with hydroxyl groups presented in the side chain of PVA. This interaction maybe confirmed by the appearance of the peak at $2\theta= 32^o$.

The average grain size of all the samples was estimated from X-ray line broadening analysis by Scherer's formula [13]

$$d = \frac{k\lambda}{\beta cos\theta} \qquad (1)$$

Where *K* represents a Scherrer's factor, λ is the X-ray wavelength, β is the value of the FWHM and θ is the Bragg's angle. The value of grain size was found to be about 26 nm for pure TiO_2 and 27nm for all the composites in average.

4.2 FTIR spectroscopy

FTIR is considered as an important tool for investigation of polymer composites structure, where it illustrates the occurrence of interaction between the various consistent according to the induced changes in the vibration modes and the band position. Fig. (2-a) shows the infrared spectrum and the assignment of the most evident absorption band of pure PVA thin film between 400-4000cm^{-1}. It appears that there is no appreciable difference in the absorption band of PVA when compared with that previously reported [14]. A broad υ (OH) absorption band is observed around 3434cm^{-1} for PVA indicating the presence of polymeric association of the free hydroxyl groups and the bounded OH stretching vibration [15]. Moreover, the few absorption peaks located between 3450-3230cm^{-1} are related to stretching band of OH hydroxyl groups that are free or bounded [16]. Two distinct absorption bands located at 2940 and 2916 cm^{-1} result from υ_{as} (CH_2) and symmetric υ_s (CH_2) stretching band of CH_2 groups respectively. Also, the shoulder peak at 2836cm^{-1} has been assignment as υ (CH) stretching vibration. The band at 1732 and 1569 cm^{-1} attributed to the stretching modes of carbonyl (C=O) group due to the residual acetate group [17]. The band 1732 cm^{-1} was observed in gamma radiolysis owing to Ketonic on acitic type carbonyl group [18]. The symmetric bending mode (CH_2) is found at 1430 cm^{-1}. The band at 1375 cm^{-1} is assigned to the mixed (CH and OH) bending modes and attributed to the associated alcohols. The band around 1257 cm^{-1} is assigned as υ_w (CH) wagging vibration. The stretching band at 1133 cm^{-1} is known to be the crystallization –sensitive band of PVA and is a measure of the degree of crystalinity [19] arises from the symmetric υ(C-C) stretching mode related to the regular repeating of the Trans – configuration of the zig zag chain in the crystalline region [20]. This band inferred that it might be due to a kind of absorption mechanism related to the presence of oxygen atom [21]. The band at 918 cm^{-1} has been related to syndiotachic structure and is assigned to rocking vibration. The band 849 and 608 cm^{-1} are assigned to υ(C-C) stretching vibration and υ (OH) out of plane (OH) bending [22].

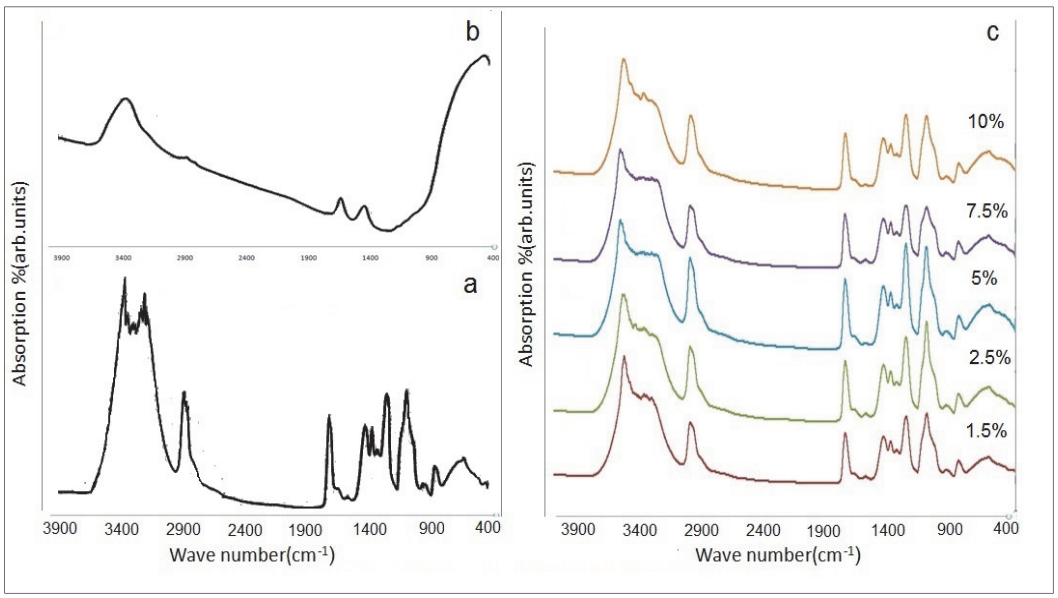

Fig. 2: Infrared spectra for (a) Pure PVA (b) Pure TiO_2 (c) TiO_2./PVA composites

Fig. (2-c) illustrates the IR spectra of TiO_2 /PVA composite films with different percentage weight ratios, the spectrum shows all the PVA peaks but with small shift and different intensity. In addition a strong broad absorption band centered at 3452 cm^{-1} was observed and it is assigned to the Ti-OH. This absorption wide band arises due to the hydrogen bonding between the OH of PVA molecules with the titanium ions Ti^{+} and allows forming charge transfer complex. These charge transfer complex suggests that number of charges must increases with increasing TiO_2. The observed changes in microstructureral properties of polymer depend on the dopant that interacts with the host polymer. The dopant serve as an electron acceptor (due to its higher electron affinity) while Polymer PVA act as an electron donor and the interaction shows a strong dependence of the donor – acceptor mechanism between the metal ion and the polymer within the composite [24] . From Fig. (2-c) one can see how much the variation of the assignment groups according to the weight ratios relative to the pure PVA. The most changed group in position and intensity is observed for OH group and the same trend is found for the groups CH binding, CH rocking, C-O stretching and Ti-O-Ti ,where these modes are shifted to forward or backward location but with less percentage than that observed for OH group . One must pay an attention to the new absorption band centered at 514 cm^{-1} which was attributed to Ti-O-O bond and all the absorption peaks that located between 450 and 600 cm^{-1} which assigned to the Ti-O-Ti bond. These peaks increase in intensity as the dopent are changed indicating that the dopant interacts considerably with the PVA molecules through two ways both or one of them .As the dopant may reside with the amorphous and/or the semi crystalline regions forming charge transfer complex or it may exist in the form of molecule aggregates between the polymer chains of PVA according to the percentage loading of TiO_2. The possibility of the interaction between TiO_2 and PVA with different percentage ratio is confirmed from the IR measurement due to the change in the fingerprint regions of the IR spectra as well as the notable changes in the shape and intensities in the region of 3000 up to 3500 cm^{-1} and the significant changes below 1000 cm^{-1}.

4.3 UV-Visible spectroscopy

The study of UV-visible absorption spectra is considered the most important tools for elucidation and understanding the electronic structure of the material under investigation through the determination of the optical band constants. Fig (3-a, b, c, d, e and f) shows the electronic absorption spectra (UV-Vis spectra) of pure PVA and TiO2 /PVA composites.

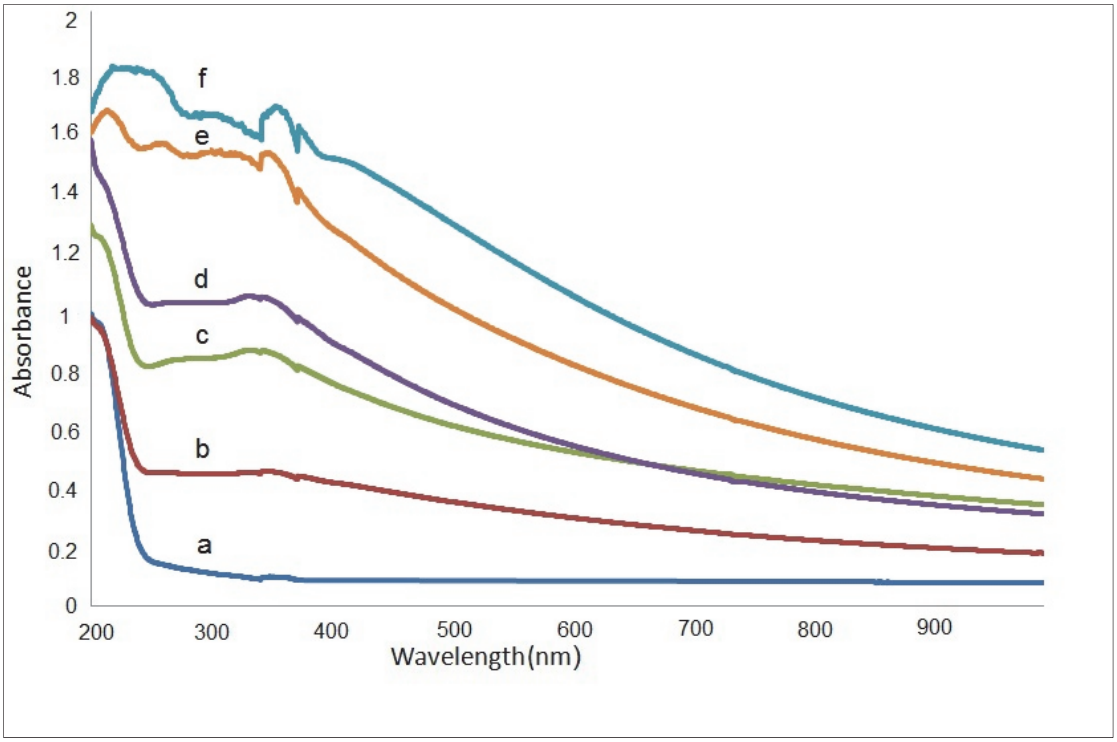

Fig. 3: UV-Visible absorption spectra for (a) Pure PVA (b) 1.5 (c) 2.5 (d) 5 (e) 7.5 (f) 10wt% TiO_2

For Pure PVA the observed absorption band at λ=198 nm is assigned for π-π^* transition and the absorption band at 281 nm is assigned to n-π^*, another shoulder peak is observed around 208 nm, these peaks indicates the presence of unsaturated bond, C=O and/or C=C mainly in the tail-head of pure PVA polymer [25], The third absorption peak is followed by a transparency region in the longer wavelengths. The anatas TiO_2 nanoparticle has an optical band gap (3.2 e.V) [41] of 388 nm. The Tio2 absorption is appeared as broadening absorption band in the TiO_2 /PVA composites, and its intensity depend upon the load of TiO_2 in the composites. Additionally the absorption peaks for the PVA are observed in all the composites .It can be noticed that the absorption increases in general with increasing dopant ratio. This observation confirming the existence of the interaction between the nanoparticles of TiO_2 with PVA and we obtained new structures for the composites of TiO_2 /PVA. This interaction occurs due to hydrogen bonding mainly between Ti ions and adjacent –OH group of PVA. Increasing the ratio of nanoparticles TiO_2, causes the UV radiation absorption edge to move towards the longer wavelength region for all the composites especially for the two samples 7.5% and 10 % weight percentage TiO_2. The transparency is good for low loading composites but not for 7.5%-10% samples. The good transparency for visible light is a particular feature of the inorganic/polymer nanocomposite certainly at low concentration, when the aggregation of the nanoparticles is inhibited. The observed irregularity in absorption of UV by the composites of high loading TiO_2

nanoparticles of percentage weight 7.5% and 10% wt/wt TiO_2 / PVA may be due to the elastic scattering of the incoming UV light upon these samples. This can happened when the particles size are smaller than the wavelength λ_{UV} (190-400 nm), or may we have an electron transition occurs in Ti^{+} ions.

The absorption coefficient α (λ) is calculated from the experimental optical absorption spectra using the relation

$$\alpha(\lambda) = \frac{1}{d} ln \frac{1}{T} = \left(\frac{2.303}{\mathrm{d}}\right) \mathrm{A} \qquad (2)$$

Where d is the film thickness, T is the transmittance and A is the absorbance. The fundamental absorption edge (E_{ed}) is considered as the lowest optical energy gap in material, it is obtained at the point where there is an abrupt rise in absorption. The absorption edge in any disordered materials follows the Urbach rule [26] given by

$$\alpha(v) = \beta \exp\left(\frac{hv}{\Delta \mathrm{E}}\right) \qquad (3)$$

Where β is constant and ΔE is the activation energy which represents the width of the tail of localized states in the forbidden gap.

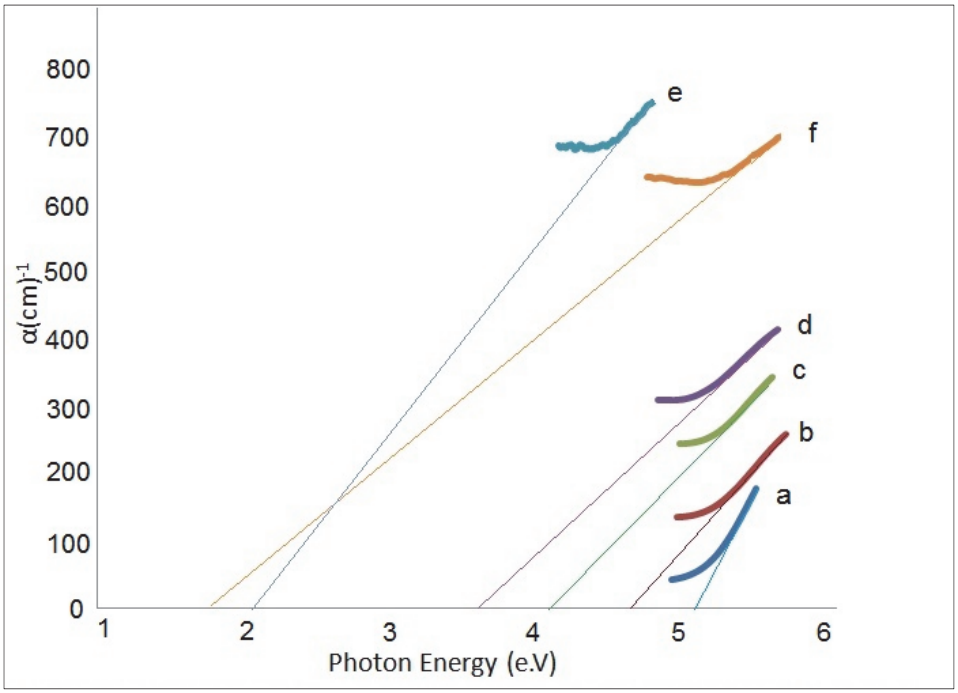

Fig. 4: Absorption coefficient as a function of Photon energy (a) Pure PVA(b) 1.5 (c) 2.5 (d) 5(e) 7.5 (f)10wt% TiO_2

Fig. (4- a, b, c, d, e , f and g) shows the dependence of the absorption coefficient on the photon energy for pure PVA, pure TiO_2 and different TiO_2/PVA composites. The absorption values increases by increasing the nanoparticles ratio which means more light absorption in higher doped films. This plot exhibit a steep rise near the absorption edge and then rapidly increase in a straight line relationship in the relatively high α region. This rapid increase of α is attributed to inter band transition with photon energy. The intercept of interpolation to zero absorption with photon energy axis was taken as the value of absorption edge that is listed in the table (1). The values of the absorption edges for the investigated samples decrease with increasing the percentage weight of the nanoparticles of TiO_2. This reduction of the absorption edge can be attributed to the changes of the

crystallinity induced by TiO_2 nanoparticles which consistent with earlier X-rays data. In addition, this may be reflecting the induced changes in the number of available final states according to the composition ratio.

The absorption tail in amorphous and semi crystalline material can be interpreted in term of the Urbach's relation (4). The band tail may be caused by many kinds of structure disorder such as point defects, alloying disorder, inhomogeneous strain, and exaction absorption and impurity level in the middle of band gap. Fig.(5-a, b, c, d, e and f) Shows the logarithmic variation of the absorption coefficient with photon energy. The relation is linear in the low energy region .The slope of the line for each case was evaluated to obtain the band tails in table (1) corresponding to each doping concentration. The values of the band tail ΔE for the composites are higher than of pure PVA, ΔE increases as the dopent ration increase. The increase of ΔE with increase doping means that the cluster size of TiO_2 nanopartiles increase i.e. there is rise in atomic densities due to the bonding between TiO_2 and pure PVA or formation of dopant aggregates lead to increase in the defect size and a modified band form could be considered . Therefore TiO_2 modified the electronic structure as well as the microstructure of PVA upon doping via deformation potential, coulomb interaction and formation localized band states [27].

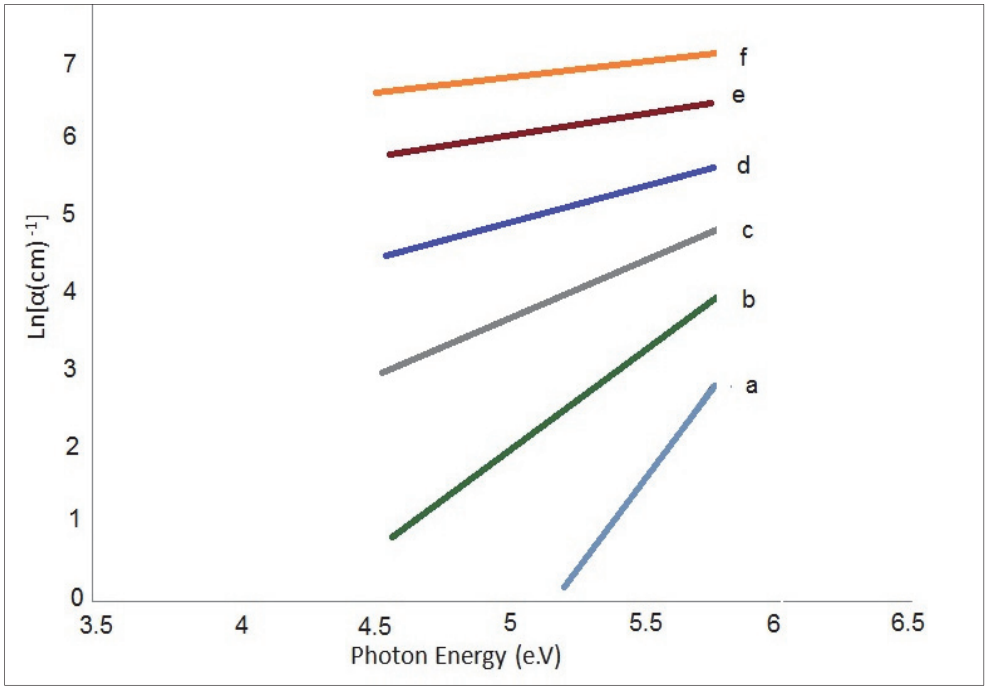

Fig. 5: Relation between Ln(α) as a function of photon energy for(a) Pure PVA (b) 1.5 (c) 2.5 (d) 5 (e) 7.5 (f)10wt% TiO_2

The absorption coefficient related for the inter-band transition near the fundamental absorption edge the Tauc equation given by [28]

$$\alpha = \frac{\beta}{h\upsilon}(h\upsilon - E_g)^m \quad (4)$$

Where hυ is the photon energy , E_g is the optical energy gap ,β is constant and m is empirical index which is equal to (2) for indirect transition as we found in TiO_2/PVA system .The spectral distribution of$(\alpha h\upsilon)^{1/2}$ for the studied sample are shown in Fig.(6-a, b, c, d, e and f). The values of the E_g of the indirect transition are obtained by extrapolating the linear region of the plot to $(\alpha h\upsilon)^{1/2}=0$. The graph representing the relation between $(\alpha h\upsilon)^{1/2}$

and hυ may be resolved into two straight lines, the straight line obtained at lower photon energy correspond to phonon absorption process and the other at higher phonon energies is due to emission process.The value of E_g for PVA pure is found to be (4.8 e.V) which is nearly similar to that calculated by other researchers (5.1 e.V) [29]and (5.05e.V) [30].Eg values for all samples are listed in table (1) .The value of E_g for pure PVA is higher than all the composites and it decreases with increasing the TiO_2 nanoparticles in the host matrix of PVA indicating the formation of some defects (additional energy levels) .These defects produce localized states in the optical band gap that increase with increasing the concentration of the defects. The lowest values of E_g are found to be corresponding to the samples 7.5% and 10% TiO_2 /PVA. Indicate clearly the changes of the microstructure as well as the electronic structure of the polymer.

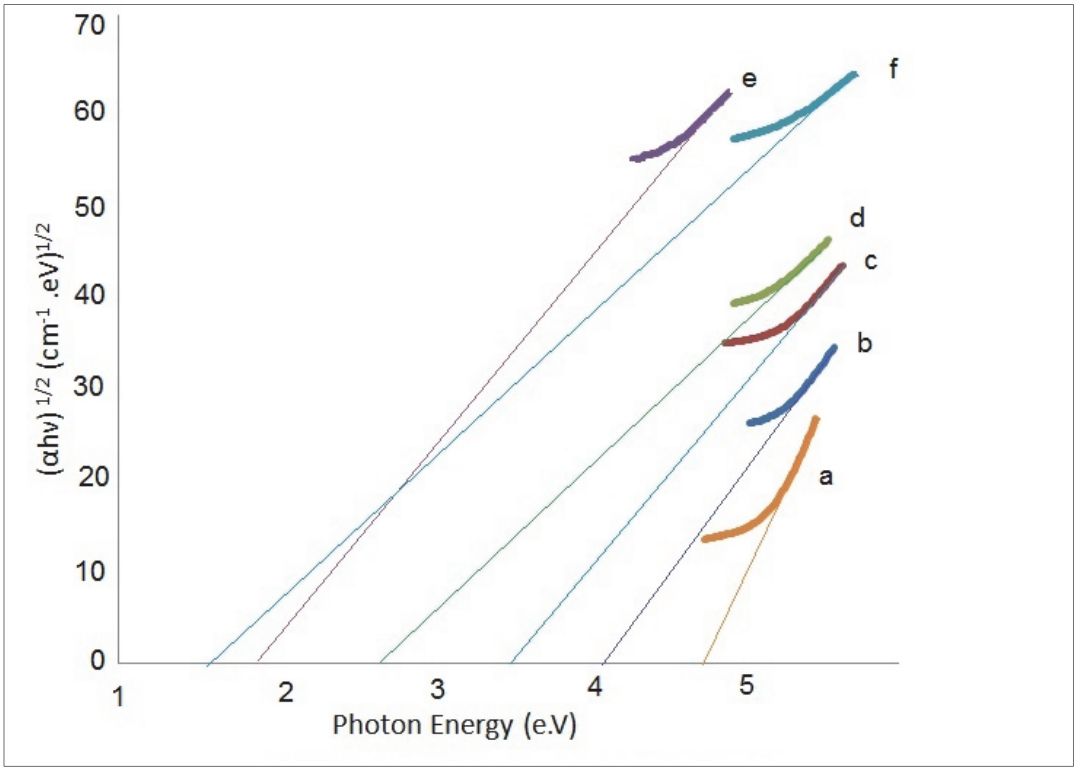

Fig. 6: The variation of (αhυ)1/2 against (hυ) for(a) Pure PVA(b) 1.5 (c) 2.5 (d) 5 (e) 7.5 (f) 10wt% TiO_2

The study of the optical constant in the vicinity of the absorption edge has yield significant information on the role of various atoms or molecules in the composite system. It is known that, if a multiple reflections are neglected, the reflectance R of the sample can be calculated from the experimental measured values of the transmittance T and absorbance using the following equation [31].

$$R = [1 - TexpA]^{1/2} \quad (5)$$

Also, the extinction coefficient k is given as

$$k = \frac{\alpha\lambda}{4\pi} \quad (6)$$

Using the values of k and R, the refractive index can be determined from the following equation [32].

$$n = \frac{(1+R) + \sqrt{4R - (1-R)^2 k^2}}{(1-R)} \tag{7}$$

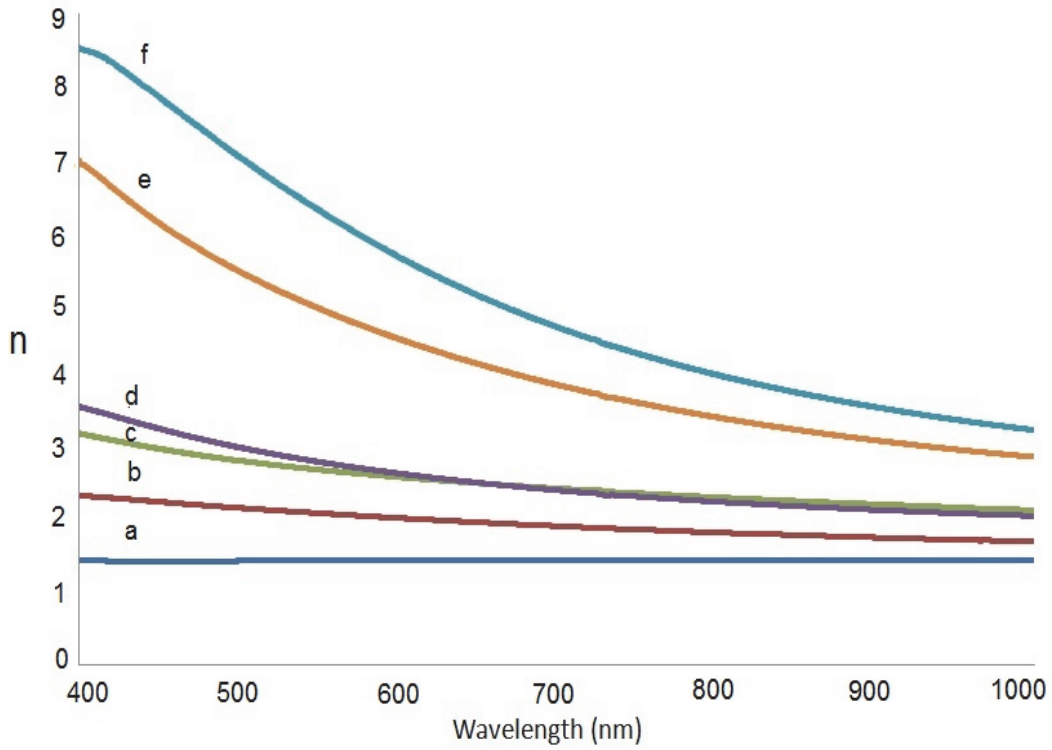

Fig. 7: Variation in refractive index (n) with wavelength for(a) Pure PVA(b) 1.5 (c) 2.5 (d) 5 (e) 7.5 (f)10 wt% TiO_2

Fig .(7-a, b, c, d, e and f) shows the n (λ) in the visible region for all the investigated samples .It is clear that the refractive index decrease slowly with increasing the wavelength showing typical shape of a dispersion curve .The value n is reached to constant n_o at longer wavelength,no(n∞) can be calculated by taking the tangent of the plotted line at the lone wavelength the intersection with the n axis is n0. The value of the refractive index of PVA is found to be (1.4) which is close to the value that is found in literature (between 1.48-1.52)[33]. The values of n_o for the composites are higher than the refractive index of pure PVA as seen in table (1). The refractive index is a fundamental property of the material, it is closely to the electronic polrizability of ions and local field inside the material. It is worth to mention that the production of high refractive index in transparent composite films is essential for development of many photonic applications such as ultra-low loss optical waveguide and more efficient given for nonlinear devices.

Table 1: Optical parameters of single oscillator for PVA and TiO_2/PVA nanocompsites

Sample TiO_2/PVA (wt/wt %)	**E_{ed}** (e.V)	**ΔE** (e.V)	**E_g** (e.V)	**n_o (1)**
0	5.1	0.2	4.8	1.4
1.5	4.7	0.4	4.2	1.9
2.5	4.3	0.8	3.5	2.4
5	3.5	1.2	2.7	2.3
7.5	2	1.4	1.8	3.6
10	1.8	1.6	1.5	4

4.4 Optical dielectric properties

One of the most optical properties is the complex dielectric function ε , which is a fundamental intrinsic property of the material
It measure the ability of a material to interact with an electric field and become polarized b y the field. The real part of the dielectric constant shows how much it will slow down the speed of light in the material and related to the stored energy within the medium, whereas the imaginary part shows how a dielectric material absorb energy from an electric field due to dipole motion .the knowledge of the real and imaginary parts of the dielectric constant provides information about the loss factor which is the ratio of the imaginary part to the real part of the dielectric constant ,the real and imaginary part of the dielectric constant can be estimated using the relation [34]

$$\boldsymbol{\varepsilon = \varepsilon_1 + i\varepsilon_2} \tag{8}$$

The real part ε_1 and the imaginary part ε_2 of this description are both frequency dependent quantities. According to the single- oscillator model [35]given by Wemple-DiDomenico, each electron is assumed to behaves as an oscillator . So, the real part of dielectric constant is expressed as

$$\varepsilon_1(\omega) = 1 + {\omega_p}^2 \sum \frac{f_n}{{\omega_n}^2 - \omega^2} \tag{9}$$

Where ω_p is the plasma angular frequency, f_n is the electrical dipole oscillator strength for the transition at frequency ω_p .

$$\omega_p = (\frac{Ne^2}{\varepsilon_0 \varepsilon_\infty m^*})^{1/2} \tag{10}$$

Where ε_∞ is the high frequency dielectric constant in the absence of any contribution from free carriers, N is the carrier concentration and m^* the effective mass ratio. For $\omega < \omega_p$ the sum over the oscillators can be separated into two parts, the dielectric constant becomes,

$$\varepsilon_1(\omega) = 1 + {\omega_P}^2 \{\frac{f_1}{{\omega_1}^2 - \omega^2} + \sum_{n \neq 1} \frac{f_n}{{\omega_n}^2}\left(1 + \frac{\omega^2}{{\omega_n}^2}\right)\} \tag{11}$$

Wemple–DiDomenico [36] had proposed that by including the higher order terms of equation (11) into the first resonant strong oscillator, the dielectric constant can be written as:

$$\varepsilon_1(\omega) = 1 + \left\{\frac{E_d E_o}{{E_o}^2 - (\hbar\omega)^2}\right\} \tag{12}$$

In this single oscillator approximation E_d is defined as dispersion energy which has a meaning of the oscillator strength of the inter-band transition and describes the dispersion of the refractive index. The other parameter E_o has a meaning of the average inter-band transition that have a straight forward relation with dipole strength. Finally, the dielectric constant for any material has been given as [32]:

$$\varepsilon_1(\omega) = n^2(h\upsilon) - 1 = \frac{E_d E_o}{{E_o}^2 - (h\upsilon)^2} \tag{13}$$

By means of these dispersion parameters, the E_d considered as a parameter having very close relation with charge distribution within unit cell and therefore with the chemical bonding given as[36]:

$$E_d = \beta N_c Z_a N_e \tag{14}$$

Where N_c is the nearest-neighbour cation coordinate number, Z_α is the formal anion valancy, N_e is the affective number of valance electrons per anion and β is constant whose value depends on the chemical bonding character of materials. β=0.26 e.V for ionic compound and 0.39ev for covalent compound [37]. Also, E_o has usually been considered as an average energy gap E_g and is empirically related to the lowest direct band gap E_g as [38]:

$$E_o \approx 1.5E_g \tag{15}$$

For further analysis of the optical data, the contribution from the free carrier electric susceptibility to the real dielectric constant is discussed according [39]:

$$\varepsilon_1 = \varepsilon_\infty - \left[\frac{e^2}{\pi c^2}\right]\left(\frac{N}{m^*}\right)\lambda^2 = -4\pi\chi_e \tag{16}$$

Where ε_∞ is the high frequency dielectric constant in the absence of any contribution from free carriers, χ_e is the dielectric free carriers susceptibility and N/m^* is the carrier concentration to the effective mass ratio (i.e. is the electronic charge) and c is the velocity of light). By drawing ε_1 as a function of λ^2 ,the relation is found to be linear the slop is equal to $(e^2/\pi c^2)(N/m^*)$ and the intersection is equal to ε_∞ .The refractive index at longer wavelength n_o is equal to $\sqrt{\varepsilon_\infty}$. It is calculated for all the samples and denoted as n_o (2) to be differentiated from the first value calculated from figure (7) .The values of calculated n_o (2) , (N/m^*) and the other constant are illustrated in table(2). Now equation (13) may be written in the form

$$(n^2 - 1)^{-1} = \frac{E_o}{E_d} - \frac{1}{E_d E_o}(h\upsilon)^2 \tag{17}$$

By plotting $(n^2-1)^{-1}$ versus $(h\upsilon)^2$ and fitting the data to the best straight line which has a negative slope$(1/E_oE_d)$ and intersection E_o/E_d. For all the investigated sample of the different weight percentage of TiO_2 nanoparticles, the estimated values of E_d and E_o are given in the table (2).

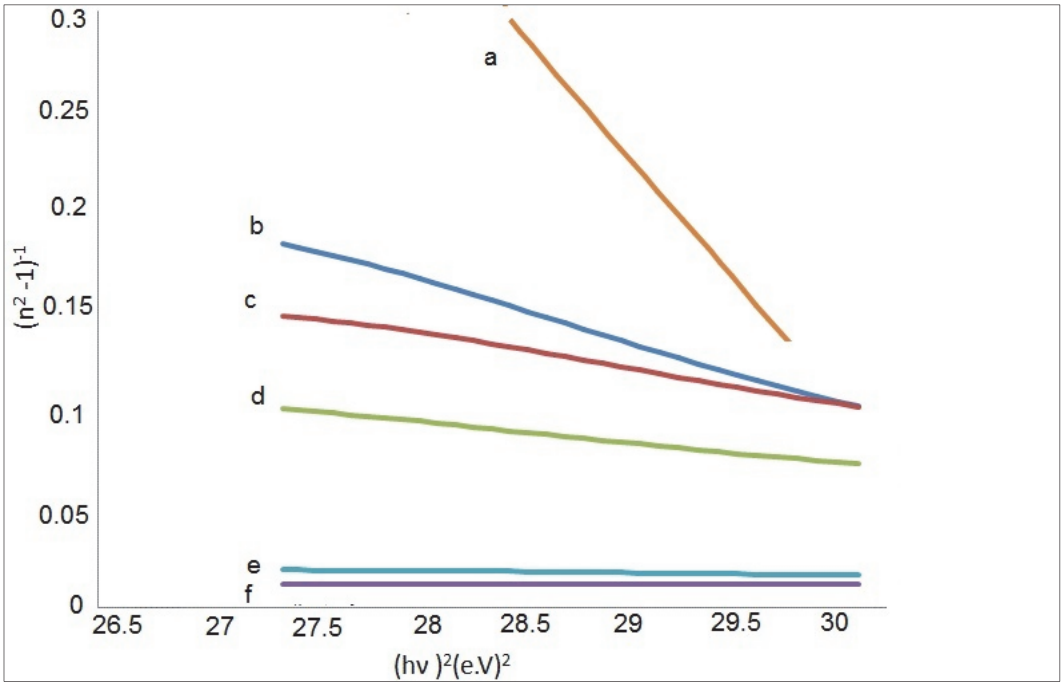

Fig. 8: Plots of (n^2-1)-1 as a function of $(h\upsilon)^2$ for (a) Pure PVA(b) 1.5 (c) 2.5 (d) 5 (e) 7.5 (f)10wt% TiO_2

One can see that the average value of oscillator energy E_o for the composite samples and PVA is in the order magnitude of $1.4E_g$, where E_g is as estimated previously in table (2). This close consistence means that the single oscillator energy E_o gives a quantitative information on the overall band structure of the material average gap and corresponds to the distance between the centre of gravity of the valence and conduction bands. The dispersion plays an important role in research for optical materials, it is a significant factor in optical communication and in designing devices. The complex refractive index (n=n+ik) and dielectric function ($\varepsilon=\varepsilon_1+ i\varepsilon_2$) are fundamental physical quantities for characterization. Real and imaginary parts of the dielectric constant are related to n and extinction coefficient k($k=\alpha\lambda/4\pi$) values by using the formula

$$\varepsilon_1 = n^2 - k^2 \quad (18)$$

$$\varepsilon_2 = 2nk \quad (19)$$

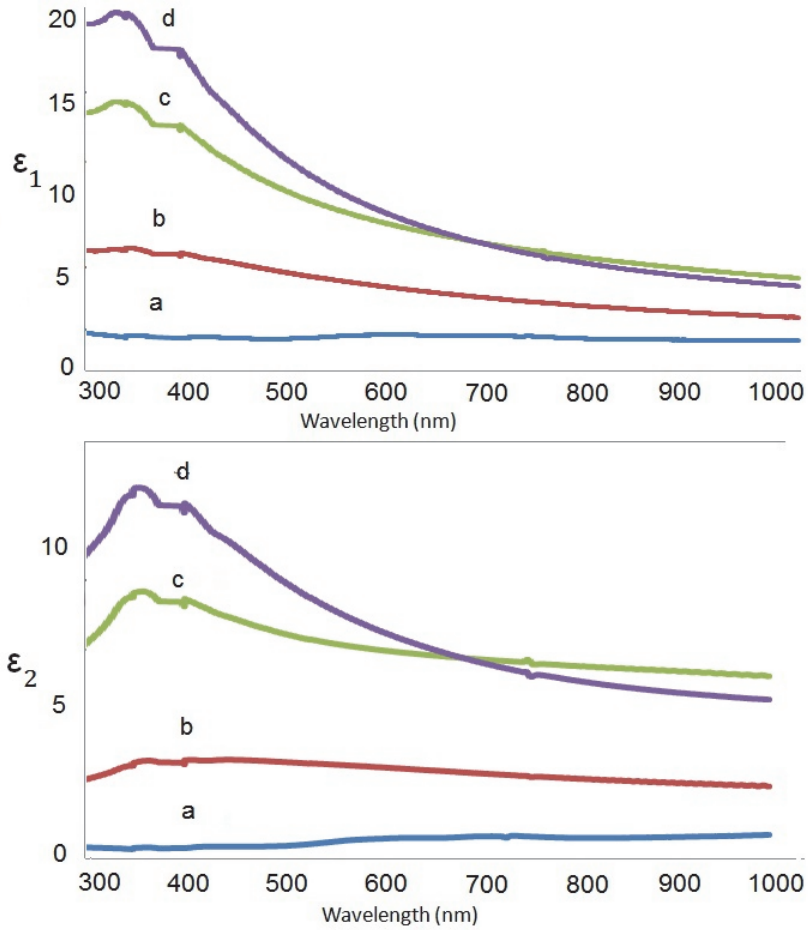

Fig. 9: The variation of ε1 and ε2 against the wavelength for (a) Pure PVA(b)1.5(c) 2.5(d) 5wt% TiO2

The variation of $\varepsilon_1$depend mostly on n^2 since k^2 is so small, while the variation of ε_2 mainly depend on k which are related to the variation of the absorption coefficient [40]

The variations of the real and imaginary parts dielectric constant with the wavelength indicate the presence of interactions between the incident photon and electrons in the composite films. This interaction is wavelength dependent, and it is attributed to the orientation of polar groups which depends on the composite types. On the other hand, the parameters of the single oscillator model E_o and E_d are related to moments of the optical spectra M_2 and M_3 through the relation given by Wemple–DiDomenico[32]as:

$$E_0{}^2 = \frac{M_2}{M_3} \tag{20}$$

$$E_d{}^2 = \frac{M_2{}^3}{M_3} \tag{21}$$

Where generally the r^{th} momentum of the optical spectrum is given by :

$$M_r = \int_{E_{g'}}^{\infty} E^{3-2r}\, \varepsilon_2(E) dE \tag{22}$$

Where E=hυ , $\varepsilon_2(h\upsilon)$ is the imaginary part of the electronic dielectric and E_g` is the lowest band gap energy . The real part ε_1 is represented by a single Sellmeier oscillator at the low energies as:

$$\varepsilon_1 - 1 = F/(E_0 - E) \tag{23}$$

F is the dipole strength related to E_o and E_d as

$$F = E_0 E_d \tag{24}$$

The single oscillator theory presents M1 as:

$$M_1 = 2\pi \int_{E_s}^{\infty} E\varepsilon_2 dE = (\,^2/_\pi\,)^2\,(\hbar w_p)^2 \tag{25}$$

Where ($\hbar\omega_p$) is the plasma energy of the valence electrons, and the average gap could be defined as:

$$E_g{}^2 = (\hbar w_p)^2/[\varepsilon_1(0) - 1\,] \tag{26}$$

Where ε_1 (0) is the static electronic dielectric constant and the combination between equation 25 and 26 yield the following expression

$$E_g{}^2 = M_1/M_2 \tag{27}$$

The calculated data in table (2) shows that the values of the spectra momentums M_1, M_2, M_3 are increasing with the increasing of TiO_2 nanoparticles within the matrix PVA.

Table 2: optical parameters of the single oscillator for PVA and TiO_2/PVA nanocompsites

Sample **TiO_2/PVA (wt %)**	$n_o(2)$	E_0 **(e.V)**	E_d **(e.V)**	M_3	M_2	M_1	**N/m***(10^{45}) Kg $^{-1}$	w_p*10^{12} e.V
0	1.3	4.9	3.4	0.029	0.69	15.98	6.3	2.9
1.5	1.8	4.3	9.6	0.12	2.23	39.38	7.8	3.3
2.5	2.3	3.63	15.6	0.326	4.29	52.64	11.2	3.9
5	2.3	2.75	11.8	0.56	4.29	31.27	14.8	4.6
7.5	3.4	1.88	19.9	2.99	10.58	34.29	16.6	4.8
10	3.8	1.62	21.8	5.13	13.46	30.27	16.8	4.9

The long wavelength refractive index n_o and the average oscillator wavelength λ_o and oscillator strength S_o parameter for the composites investigated samples can be determined by the single oscillator model as:

$$\frac{(n_o{}^2 - 1)}{(n^2 - 1)} = 1 - \frac{\lambda_o{}^2}{\lambda^2} \tag{28}$$

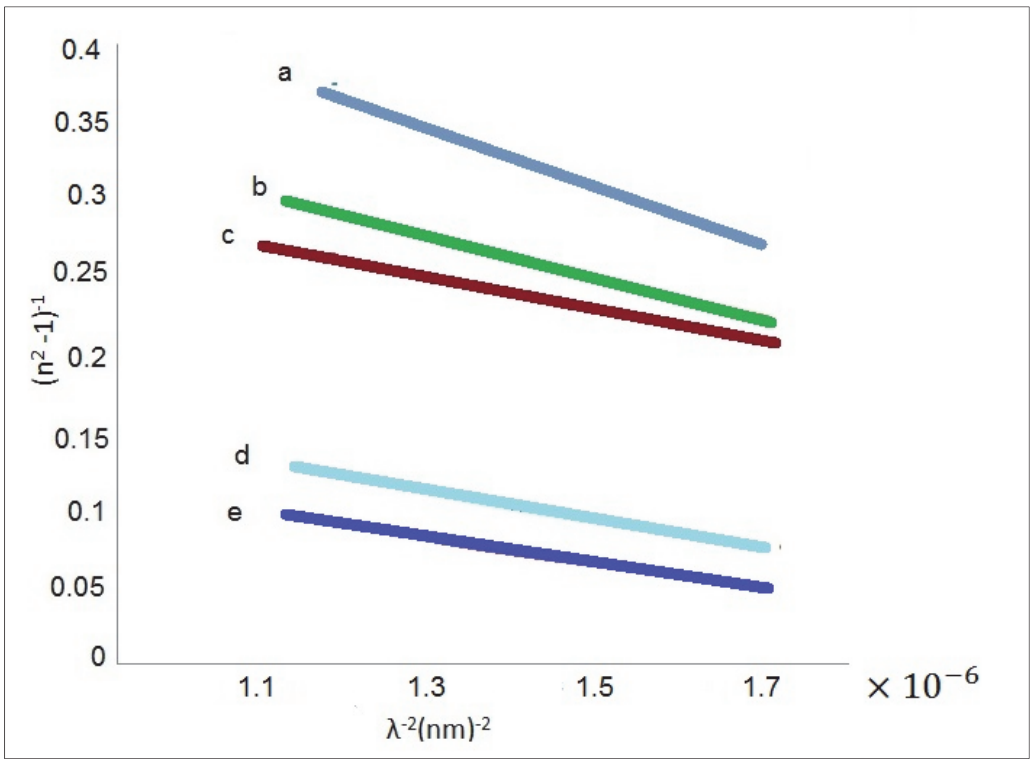

Fig. 10: Relation between $(n^2-1)^{-1}$ and λ^{-2} for (a) Pure PVA(b) 1.5 (c) 2.5(d) 5(e) 7.5 wt%TiO_2

The $n_o(3)$ values for the composite films was obtained from the linear part of the curve of $(n^2-1)^{-1}$ Vs λ^{-2}, taken below the absorption edge, as shown in Fig. (10- a, b, c, d, and e) The intersection with $(n^2-1)^{-1}$axis is $(n_o^2-1)^{-1}$ and n_o^2 at λ_o equal to ε_∞ (high frequency dielectric constant) .

Rearranging equation (28) gives [39]:

$$(n^2-1)=\frac{S_0\lambda_0}{1-(\frac{\lambda_0}{\lambda})^2} \tag{29}$$

Where ($S_o = n_o^2/\lambda_o^2$) is the average oscillator parameter, which is the strength of the individual dipole oscillator. The values for (3) S_o, λ_o and ε_∞ are indicated in the table 3.

Table 3: single oscillator parameter of Pure PVA and TiO_2 nanocomposites

Sample TiO_2/PVA (wt/wt %)	(λ_0) (nm)	$\boldsymbol{\varepsilon_\infty}$ (F/m)	$\mathbf{S_o}$ (10^5) (nm^{-1})	$\boldsymbol{n_0}(3)$
0	110	1.82	6.79	1.35
1.5	421	3.5	1.41	1.87
2.5	443	5.34	2.23	2.32
5	450	5.57	2.26	2.36
7.5	522	12.3	4.13	3.5
10	544	15.2	4.8	3.9

It can be seen from the table (3). the refractive index n_o (3) calculated from the single oscillator model is close to the previously calculated values n_o (2) and n_o (3). The value of ε_∞ increases with increasing TiO_2 .This means that the lattice vibration and bounded carriers varies with different concentration of TiO_2 nanopartlices.

5. Conclusion

- The spectroscopic investigation revealed that the Ti+ ions of the dopant interacts with OH groups of PVA and forms a complex via intra/inter molecules hydrogen bonding. The microstructure changes due to complex formation observed through the investigation of the spectra of X-ray diffraction IR and UV-Vis spectra for different content of TiO_2 nanoparticles in PVA.
- The decreasing of the optical energy gap depends upon the increasing of the dopant content.
- The refractive index is found to be enhanced with increase the dopant content. The increase of n for higher doped PVA films is significant for material that could be used for fabrication of optical waveguides and photonic circuits.
- In term of the Tauc method and Wample DiDominco model, the optical band gap E_g and the average inter-band transition energy E_o were found in good agreement for the type of indirect transition.
- Values of the dielectric constant are higher than the imaginary part.
- The moments M_2 and M_3 are increase with TiO_2 accordingly the dispersion energy E_d fellow the same trend.
- Finally titanium oxide nanopartices plays an important role in modification of the optical and dialectical properties of PVA to make it more applicable.

References

[1] Chahal, R.P., Mahendia, S., Tomar, A.K. and Kumar, S., Alloys Compd **538** (2012) 212-219.
[2] Wu, W., Liang, S., Shen, L., Ding, Z., Zheng, H., Su, W. and Wu, L., Alloys Compd., **520** (2012) 213-219
[3] Kinadjian, N.; Achard, M.-F.; Julián-López, B.; Maugey, M.; Poulin, P.; Prouzet, E.; Backov, R. Adv. Funct. Mater **22** (2012) 3994–4003
[4] A.H. Yuwono, J. Xue, J. wang ,H.I. Elim , and Wei Ji ., Nonlinear Optical Physics and Material **14** (2005) 281-297
[5] S.Lewis, V. Hayns, R.Wheeler-Jones,J.Sly, R.M.Perks, L.Piccirillo, Thin solid films **518** (2010)2683-2687.
[6] A.Matilainen,M.Sillanpaa, Chemosphere **80** (2010)351-365.
[7] M.Wouters, C.Rentrop, P.Willemsen, Progress in Organic Coating **68** (2010) 4-11
[8] W.Su, S.Wang, X.Wang, X.Fu, J.Weng, Surface and Coating Technology. **205** (2010) 465-469
[9] Torres-Sanchez, C.; Corney, Ultrasonics Sonochemistry **15** (4) (2008), 408-415.
[10] Xinhua Yuan , Zhiwei Tian, Advanced Martial Letters **1** (2)(2010) 135-142
[11] M.Abdelaziz, Magdy M. Ghannam, Physica **B 405** (2010) 958-964.

[12] Song, Y Zhang J, Yang H Xu, S Jiang, L Dan Y, Appl.Surface Science **292** (2014) 978-985.
[13] Jia-Guo Yu, Xiu-Jian Zhao, Huo-Gen Yu, Bei Cheng, Wing-Kei Ho, physical chemistry **B 107** (50) (2003) 13871-13879.
[14] Y.M.Lee, S .H.Kim and S.J.Kim, Poymer **37** (26) (1996) 5897-5905.
[15] P.Sakellariou, A.Hassan and R.C.Rowe, Polymer **34** (6) (1993) 1240-1248.
[16] S.Krimm,C.Y.Liang and G.BB.M.Sutherlond, Polymer. Science **22**(1956) 227-247
[17] A.Danno, Physical Society of Japan., **13** (6)(1958) 609-613.
[18] M.Tadokoro, S.Seki and I.Nitta,Bull.Chem.Soc.Jpn., **28** (1959), 559-564.
[19] J.F.Kenney and G.W.Willcockson, Polym.Sci. **A-1** (4) (1966) 679-698
[20] H.Tadokoro,S.Seki and I.Nitta,Bull. Chem.Soc.Jpn **22**(1957) 563
[21] A.Elliott, E.J.Ambrose and R.B.Temple, Chem.Phys **16** (1948)877
[22] M. Sivabalan, V. Gayathri, C. Kiruthika and B. Madhan, International Journal of Pharmacy and Technology **4** (2) (2012) 4493–4505,
[23] Gao,Y.; Masuda,Y.; Peng,Z.;Yonezawa,T.; Koumoto,K., Mater. Chem **13** (2003) 608-613
[24] M.P.F.Garaca,C.C.Silva,L.C.Costa,M.A.Valente, Int.J.nanoelectronics and materials 3 (2010) 99-111
[25] J.H.Bang, K.S.Suslick, Adv.Mater. **22** (2010) 1039-1059
[26] S.D. Praveena, V. Ravindrachary, R.F. Bhajantri and Ismayi (2014) Dopant induced microstructural, optical, and electrical properties of TiO2/PVA composite. Polym Compos. **doi: 10.1002/pc.23258**
[27] A.E. Shalan, M.M. Rashada, Youhai Yu, Monica Lira-Cantu, M.S.A. Abdel-Mottaleb ,Electrochimica Acta **89** (2013) 469– 478
[28] R.M. Radwan, J. Phys. D: Appl. Phys **42** (2009) 015419
[29] M.G. Sandoval-Paz, M.sotelo-Lerma, J.J.Vaenzuela-Jauregui, M-Fores Acosta, R.Ramirez-Bon,Thin Solid Films **472** (2005) 5-10
[30] K.Thyagarajan, International Journal of Engineering Research and Development, 6, 8 (2013) 15-18
[31] Z. Raheem, IJAIEM, 2, 10 (2013) 2319 – 4847
[32] N.F. Mott and N.F. Davis, Electronic Process in Non- Crystalline Materials, 2nd ed. USA, Oxford University Press (1979).
[33] M. DiDomenico, S.H. Wemple, J. Appl. Phys. **40** (1969) 720-723
[34] Dmitry A. Yakovlev, Vladimir G. Chigrinov, Hoi-Sing Kwok, Modeling and Optimization of LCD Optical Performance , John *Wiley* & Sons Ltd (2015)
[35] *A. Goswami*, *Thin Film Fundamentals*, *New Age International* (P) Ltd. Publishers, *(2005)*
[36] M. Caglar, M. Zor, S. Ilican, Y. Caglar, Czech. J. Phys 56 (2006) 277-281.
[37] S.H.Wemple and DiDomenics:Phys.Rev **B** (3) (1971) 1338 -1352
[38] E. Marquez, J.B. Ramirez-Malo, P. Villares, R. Jimenez-Garay, R. Swanepoel, Thin Solid Films **254** (1995) 83-87
[39] M.B. El-Den, M.M. El-Nahass, J. Opt. Laser Technol. **35** (2003)335-340
[40] S. H. Wemple, M. DiDomenico, Phys. Rev. Lett. **23** (1969) 1156-1160
[41] A.Q.Abdullah, S.S.El-Lauibi,E.M. Jaboori,Int.J.nanoelectronics and materials 7 (2014) 65-76